Eur. Phys. J. B **4**, 113–119 (1998)

THE EUROPEAN PHYSICAL JOURNAL B

Electron–phonon scattering in an asymmetric double barrier resonant tunneling structure

J.-J. Shi[a], B.C. Sanders[b], and S.-H. Pan[c]

School of Mathematics, Physics, Computing and Electronics, Macquarie University, Sydney, New South Wales 2109, Australia

Received: 23 December 1997 / Revised: 24 March 1998 / Accepted: 9 March 1998

Abstract. We calculate the electron-phonon scattering rate for an asymmetric double barrier resonant tunneling structure based on dielectric continuum theory, including all phonon modes, and show that interface phonons contribute much more to the scattering rate than do bulk-like LO phonons for incident energies which are approximately within an order of magnitude of the Fermi energy. The maximum scattering rate occurs for incident electron energies near the quantum well resonance. Subband nonparabolicity has a significant influence on electron-phonon scattering in these structures. We show that the relaxation time is comparable to the dwell time of electrons in the quantum well for a typical resonant tunneling structure.

PACS. 72.10.Di Scattering by phonons, magnons, and other non localized excitations – 63.20.Kr Phonon-electron and phonon-phonon interactions

1 Introduction

The Double Barrier Resonant Tunneling Structure (DBRTS) [1,2] is interesting for both scientific and technological reasons. At a fundamental level the DBRTS provides a system for testing theories of electron transport, tunneling and scattering. The DBRTS also offers the advantages of negative differential resistance, high-frequency oscillations and rapid switching [3,4]. The rapidly developing field of eptixial growth has rejuvenated interest in DBRTS as increasingly high-quality structures are being fabricated.

The property of negative differential resistance is particularly useful, allowing rapid switching. A resonant tunneling diode is characterised by a current-to-voltage characteristic curve, and, for a resonant bias voltage v_0, a peak exists in this characteristic curve. For a bias voltage $v > v_0$, the slope of this curve is negative, and the degree of negative resistance is quantified by the Peak-to-Valley Ratio (PVR) of the resonance peak. Understanding the valley current is thus quite important for designing better DBRTS.

In general, the valley current can be caused by several process, including elastic scattering of tunneling electrons both by impurities and by interface roughness, quasielastic scattering by acoustic phonons, resonant $\Gamma - X$ intervalley tunneling and inelastic scattering by optical phonons [5]. In particular mechanisms of electron-phonon interactions and scattering in polar semiconductor DBRTS are being investigated because of their important contribution at high temperatures ($T > 40$ K). Phonon-assisted tunneling in symmetric DBRTS has been widely investigated. The first experimental proof of scattering in the valley current was given by Goldman, Tsui, and Cunningham [6], who observed a Longitudinal Optical (LO) phonon satellite in the current-voltage characteristics of a GaAlAs double barrier diode. Wingreen, Jacobsen and Wilkins [7] calculated the tunneling current through a resonant tunneling structure including electron-phonon interaction in the Quantum Well (QW) using independent boson models, and found a sideband in the valley region of the tunneling current.

The current-voltage characteristics of DBRTS are investigated in the presence of a quantizing magnetic field perpendicular to the barriers in reference [8]. Jonson [9] solved an approximate model for inelastic resonant tunneling in the presence of a boson field. Cai *et al.* [10] investigated one-dimensional electron tunneling in an arbitrarily shaped barrier in the presence of electron-optical-phonon scattering. Chevoir and Vinter [11] calculated the LO phonon scattering contribution to electron tunneling through a double barrier diode. Wingreen *et al.* [12] further investigated resonant tunneling transmission probability for an electron interacting with phonons and inelastic scattering in resonant tunneling structures. Turley and Teitsworth [13,14] studied optical phonon modes, electron-phonon interaction, and phonon-assisted tunneling in symmetric DBRTS in detail. The effects of electron-interface-phonon interaction on resonant

[a] e-mail: shijj@jen.mpce.mq.edu.au
[b] e-mail: barry.sanders@mq.edu.au
[c] *Permanent address:* Institute of Physics, Chinese Academy of Sciences, P.O. Box 603, Beijing 100080, P.R. China.
e-mail: shp@aphy02.iphy.ac.cn

tunneling in symmetric double barrier heterostructures have also been studied in reference [15]. The inelastic scattering effect on electron tunneling through a double barrier resonant tunneling device was also studied by Zou and Chao [16]. The effects of localized phonon modes on the current-voltage curves of DBRTS have also been calculated in the presence of large magnetic fields parallel to the applied electric field in reference [17]. Moreover, a coupled double-quantum-well resonant tunneling structure in the presence of electron-phonon interaction was also investigated carefully in reference [18].

Recently, asymmetric heterostructures, such as asymmetric DBRTS and asymmetric QW structures, have generated interest due to their special device applications [19–26]. Optical-phonon modes, electron-phonon interaction and scattering, and polaron effects in asymmetric QW have been investigated in references [19–21]. Some important results, such as the frequency-forbidden behavior of the interface optical phonon modes and the anomalous phenomenon of the electron-phonon interaction in asymmetric QW, have been found [19,20]. Some investigations further indicate that the negative differential resistance can be tuned when asymmetric barriers are used in tunneling structure [22]. Asymmetric double barrier heterostructure may vary the amount of charge accumulation in the QW so that the current-voltage characteristics can be modified [23,24]. Asymmetric tunneling structures may enhance the resonant peak current [25]. However, to our knowledge, little work has been done about electron-phonon interaction and scattering and phonon-assisted tunneling in asymmetric DBRTS in the presence of electron-phonon interaction in theory, despite its great theoretical and practical importance at present. Hence it is worthwhile investigating electron-phonon interaction and scattering and phonon-assisted tunneling in asymmetric DBRTS. The main purpose of this paper is to calculate electron-phonon interaction and scattering rates in asymmetric DBRTS using the dielectric continuum model. Both interface and confined bulk-like LO phonons are incorporated. The conduction band nonparabolicity is also considered. We show that interface phonons contribute more significantly than do bulk-like phonons for low incident electron energies as well as establishing the importance of subband nonparabolicity in these calculations. We also establish a relationship between the electron dwell time in the resonant tunneling structure and the relaxation time for the system. These results are important for analyzing and understanding scattering processes and decoherence in DBRTS and in device applications of resonant tunneling diodes.

2 Theory

2.1 Transmission probability and electron wavefunctions across arbitrary potential field

The conduction band edge of DBRTS is curved for a nonzero bias voltage due to the accumulation of electrons in the QW *via* resonant tunneling; hence the potential function $v(z)$ has a complicated form. In order to solve the electron states in this complicated potential field, let us now consider an arbitrary potential field $v(z)$ within the region $0 \le z \le L$ in the z direction. The transfer-matrix method is used to solve the single-electron effective-mass Schrödinger equation effectively for arbitrary $v(z)$. The transmission probability and electron envelope wavefunctions can be obtained conveniently. Our methods are briefly summarized as follows.

First, we select an integer $N > 0$ and divide the interval $[0, L]$ into N equal subintervals with the same length $a = L/N$. Because the potential may be treated as constant over each subinterval as long as the length a is very small, for instance, 5 Å in GaAs, the solution of the one-dimensional Schrödinger equation is given in the jth subinterval as a superposition of plane waves:

$$\psi_j(z_j) = A_j \exp(k_j z_j) + B_j \exp(-k_j z_j), \qquad (0 \le z_j \le a), \tag{2.1}$$

where the first term is for left-to-right transfer, and the second for right-to-left. The z component of the complex wave vector, k_j, in equation (2.1) is given by

$$k_j = \left[\frac{2m_j(E_z)(v_j - E_z)}{\hbar^2}\right]^{1/2}, \qquad j = 1, 2, \cdots, N. \tag{2.2}$$

Here E_z is the electron energy in the z direction. v_j and $m_j(E_z)$ are the potential and the effective mass associated with subinterval j, and z_j is distance measured from the left-hand side of the jth subinterval. The j values increase as the structure is traversed from the left ($z = 0$) to the right ($z = L$). Including the subband nonparabolicity, the electron effective mass $m_j(E_z)$ can be given as [21]

$$m_j(E_z) = m_j[1 - (v_j - E_z)/E_{gj}], \tag{2.3}$$

where E_{gj} is the energy gap between the conduction and the light-hole valence bands in the jth subinterval. The electron band mass m_j is constant in the jth subinterval.

Using the Bastard [27] boundary conditions at the boundary between subintervals j and $j+1$, one can derive the following matrix formula relating successive A and B plane-wave coefficients, namely,

$$\begin{pmatrix} A_{j+1} \\ B_{j+1} \end{pmatrix} = M_j \begin{pmatrix} A_j \\ B_j \end{pmatrix}, \tag{2.4}$$

where the matrix M_j is defined as

$$M_j = \frac{1}{2}\begin{pmatrix} (1+\alpha_j)\exp(k_j a) & (1-\alpha_j)\exp(-k_j a) \\ (1-\alpha_j)\exp(k_j a) & (1+\alpha_j)\exp(-k_j a) \end{pmatrix}, \tag{2.5}$$

with

$$\alpha_j = \frac{k_j m_{j+1}(E_z)}{k_{j+1} m_j(E_z)}\,. \tag{2.6}$$

From equations (2.1–2.6), we obtain the electron envelope wavefunction in the entire region $[0, L]$ if the coefficients A_1 and B_1, or equivalently, A_N and B_N, are known.

The plane-wave coefficients A_1 and B_1 in the first subinterval and the coefficients A_N and B_N in the Nth subinterval have the following matrix relation:

$$\begin{pmatrix} A_N \\ B_N \end{pmatrix} = M_{tot} \begin{pmatrix} A_1 \\ B_1 \end{pmatrix}, \tag{2.7}$$

where

$$M_{tot} = \begin{pmatrix} M_{11} & M_{12} \\ M_{21} & M_{22} \end{pmatrix} = M_{N-1} \cdot M_{N-2} \cdots M_2 \cdot M_1. \tag{2.8}$$

One can prove from equations (2.5, 2.8) the following results

$$\begin{aligned} &\det(M_j) = \alpha_j, \\ &\det(M_{tot}) = \alpha_{N-1} \cdot \alpha_{N-2} \cdots \alpha_2 \cdot \alpha_1 = \frac{k_1 m_N(E_z)}{k_N m_1(E_z)}. \end{aligned} \tag{2.9}$$

The above equations (2.1–2.9) are universal for an arbitary potential field. Let us now briefly discuss their applications for electron tunneling through asymmetric DBRTS in two important cases.

2.1.1 Emitter-to-collector tunneling

The solution of the Schrödinger equation in the $j = 1$ subinterval can be written as

$$\psi_1(z_1) = A_1 \exp(k_1 z_1) + B_1 \exp(-k_1 z_1). \tag{2.10}$$

For left-to-right transfer, we can assume $A_1 = 1$ and $B_N = 0$ for convenience. Thus, we have

$$\psi_N(z_N) = A_N \exp(k_N z_N), \tag{2.11}$$

and

$$\begin{pmatrix} A_N \\ 0 \end{pmatrix} = \begin{pmatrix} M_{11} & M_{12} \\ M_{21} & M_{22} \end{pmatrix} \begin{pmatrix} 1 \\ B_1 \end{pmatrix}. \tag{2.12}$$

We can obtain from equation (2.12)

$$\begin{aligned} A_N &= \frac{\det(M_{tot})}{M_{22}} = \frac{k_1 m_N(E_z)}{k_N m_1(E_z)} \frac{1}{M_{22}}, \\ B_1 &= -\frac{M_{21}}{M_{22}}. \end{aligned} \tag{2.13}$$

The transmission probablity $T(E_z)$, which is defined as the ratio of the transmitted particle flux divided by the incident particle flux, is given by

$$T(E_z) = \frac{m_N(E_z) \mid k_1 \mid}{\mid k_N \mid m_1(E_z)} \frac{1}{\mid M_{22} \mid^2}. \tag{2.14}$$

The electron envelope wavefunction $\psi(z)$ can be normalized according to the following formula

$$\int_0^L \mid \psi(z) \mid^2 dz = 1. \tag{2.15}$$

2.1.2 Collector-to-emitter tunneling

In this case, we can assume $A_1 = 0$ and $B_N = 1$ for convenience. The solutions of the Schrödinger equation in the $j = 1$ and $j = N$ subintervals are given as

$$\begin{aligned} &\psi_1(z_1) = B_1 \exp(-k_1 z_1), \\ &\psi_N(z_N) = A_N \exp(k_N z_N) + \exp(-k_N z_N). \end{aligned} \tag{2.16}$$

The coefficients A_N and B_1 can be determined as follows,

$$\begin{aligned} A_N &= \frac{M_{12}}{M_{22}}, \\ B_1 &= \frac{1}{M_{22}}, \end{aligned} \tag{2.17}$$

and the transmission probability $T(E_z)$ satisfies formula (2.14). Normalization of the electron envelope wavefunction $\psi(z)$ is established by equation (2.15).

2.2 Electron-phonon interaction and scattering in asymmetric DBRTS

Within the framework of the dielectric continuum model, optical phonon modes and electron-phonon interaction Fröhlich-like Hamiltonian H_{e-ph} can be conveniently obtained. The electron-phonon scattering rate W can be calculated according to the Fermi golden rule. For an asymmetric DBRTS we can obtain the scattering rate due to interface phonons as follows

$$\begin{aligned} W^{(i\to f)}(\mathbf{k}_i, E_z) = &\frac{e^2}{16\pi\varepsilon_0} \sum_m \int d^2\mathbf{k} \frac{1}{\omega_m(k) k} \mid F_m(k) \mid^2 \\ &\times \delta(\varepsilon_i - \varepsilon_f \pm \hbar\omega_m(k)) \left(N_{ph} + \frac{1}{2} \mp \frac{1}{2} \right) \delta_{\mathbf{k}_i, \mathbf{k}_f \mp \mathbf{k}}, \end{aligned} \tag{2.18}$$

and the rate due to confined LO phonons is

$$\begin{aligned} W^{(i\to f)}(\mathbf{k}_i, E_z) = &\frac{e^2}{2\pi\varepsilon_0} \sum_\nu \sum_{j=1}^{j_{max}} \frac{\omega_{L\nu}}{T_\nu} \\ &\times \left(\frac{1}{\epsilon_{\infty\nu}} - \frac{1}{\epsilon_{0\nu}} \right) \mid F_{if}(q_\nu^j) \mid^2 \\ &\times \int d^2\mathbf{k} \frac{1}{k^2 + (q_\nu^j)^2} \delta(\varepsilon_i - \varepsilon_f \pm \hbar\omega_{L\nu}) \\ &\times \left(N_{ph} + \frac{1}{2} \mp \frac{1}{2} \right) \delta_{\mathbf{k}_i, \mathbf{k}_f \mp \mathbf{k}}, \end{aligned} \tag{2.19}$$

where N_{ph} is the phonon occupation number and can be determined by the Planck distribution [28] as

$$N_{ph} = \frac{1}{\exp(\hbar\omega_p / k_B T) - 1}. \tag{2.20}$$

Here $\hbar\omega_p$ is the phonon energy, T is the temperature and k_B is Boltzmann's constant. In equations (2.18, 2.19),

the upper sign is for phonon absorption and the lower is for emission, and $F_m(k)$ and $F_{if}(q_\nu^j)$ are the overlap integrals defined as

$$F_m(k) = (\Lambda\Delta^2)^{-1/2} \int_\Omega \psi_f^*(z) f_m(k,z) \psi_i(z) dz, \quad (2.21)$$

where Ω refers to the entire DBRTS region, and

$$F_{if}(q_\nu^j) = \int_{layer\ \nu} \psi_i(z) \sin\left[q_\nu^j (z - z_{0\nu})\right] \psi_f^*(z) dz, \quad (2.22)$$

with ε_i and ε_f the energies of the initial and final electron states, respectively. We designate ψ_i and ψ_f as the electron envelope wavefunctions in the initial and final states. For phonon-assisted tunneling, ψ_i can be calculated according to the transfer-matrix method described in Section 2.1. Since the width of the final resonant state is very narrow, we can treat the final state as a completely localized state in the well [11,13,14,29]. The electron energy ε can be written as the sum of parallel and transverse components:

$$\varepsilon = \frac{\hbar^2 k_e^2}{2m^*} + E_z. \quad (2.23)$$

The above equations are exact and show that scattering rates are functions of the in-plane wave vector $\mathbf{k}_i$ and energy E_z in the z direction of the initial electron state.

Since the electron is constrained to move along the z direction and its motion in the plane of the interfaces will be suppressed due to nonzero bias voltage in the z direction in DBRTS, the electron energy E_z in the z direction is significantly larger than the energy $E_\parallel = \hbar^2 k_i^2 / 2m^*$ in the plane of the interfaces, where $\mathbf{k}_i$ is the in-plane wave vector. For simplicity, we can assume that the electron energy $E_\parallel$ is small relative to E_z. In this case, it has been shown from the theory that the scattering rate $W(\mathbf{k}_i, E_z)$ depends weakly on $\mathbf{k}_i$ [13]. The weak dependence of $W(\mathbf{k}_i, E_z)$ on $\mathbf{k}_i$ has also been further discussed for confined phonon modes in reference [14]. The scattering rate $W(\mathbf{k}_i, E_z)$ depends strongly on E_z since the overlap integral F_m or F_{if} has a sensitive E_z dependence. On the contrary, $\mathbf{k}_i$ only occurs in the delta function, and then gives an indirect influence on F_m or F_{if}. We thus have $W(\mathbf{k}_i, E_z) \doteq W(0, E_z) \equiv W(E_z)$. For phonon-assisted tunneling in an asymmetric DBRTS, the scattering rate $W(E_z)$ for phonon emission can be calculated according to the formula,

$$W(E_z) = \frac{e^2}{8\varepsilon_0} \sum_{m=1}^{8} \frac{1}{\omega_m(k_p)} |F_m(k_p)|^2 \times \left(\left| \frac{\hbar^2}{m^*} k_p + \hbar \left. \frac{d\omega_m}{dk} \right|_{k=k_p} \right| \right)^{-1} (N_{ph} + 1), \quad (2.24)$$

where k_p satisfies

$$\frac{\hbar^2}{2m^*} k_p^2 + \hbar\omega_m(k_p) - (E_z - E_w) = 0 \quad (2.25)$$

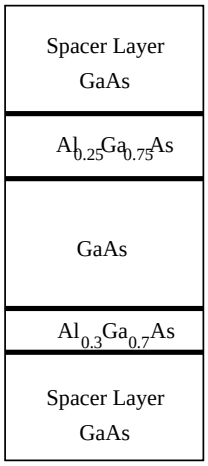

Fig. 1. Asymmetric double barrier resonant tunneling structure GaAs/$Al_{0.25}Ga_{0.75}As$/GaAs/$Al_{0.3}Ga_{0.7}As$/GaAs with thickness 1000 Å/30 Å/60 Å/20 Å/1000 Å.

for interface phonons. Similarly the scattering rate for confined bulk-like LO phonon emission,

$$W(E_z) = \frac{m^* e^2}{\hbar^2 \varepsilon_0} \sum_{\nu=2,3,4} \sum_{j=1}^{j_{max}} \frac{\omega_{L\nu}}{T_\nu} \times \left(\frac{1}{\epsilon_{\infty\nu}} - \frac{1}{\epsilon_{0\nu}} \right) \frac{|\ F_{if}(q_\nu^j)\ |^2}{(k_p^\nu)^2 + (q_\nu^j)^2} (N_{ph} + 1), \quad (2.26)$$

with

$$k_p^\nu = [2m^*(E_z - E_w - \hbar\omega_{L\nu})]^{1/2} / \hbar. \quad (2.27)$$

In equations (2.25, 2.27), $(E_z - E_w)$ is the energy difference between the incident state and the final resonant state localized in the well. The definitions of q_ν^j, T_ν, Λ, Δ, $f_m(k,z)$, and $z_{0\nu}$, provided in reference [20], are lengthy and not repeated here. Electron-phonon scattering in the emitter and collector regions have been ignored because the overlap integrals between the emitter (collector) and the final localized resonant state in the well are negligible.

3 Numerical results and discussion

As an application of our theory given in Section 2, we have performed numerical calculations for the transmission coefficient $T(E_z)$, electron envelope wavefunction and electron-phonon scattering rate W corresponding to the asymmetric DBRTS shown in Figure 1. We employ the physical parameters obtained in reference [19] and the energy gap $E_g = 1424 + 1266x + 260x^2$ meV for $Al_xGa_{1-x}As$ material.

Figure 2 shows the transmission coefficient $T(E_z)$ as a function of the incident electron energy E_z for the different bias voltages $v = 0$, 150 and 200 mV, respectively. We can see from Figure 2 that there are two transmission peaks which are localized at $E_z = 57.5$ and 233.6 meV for

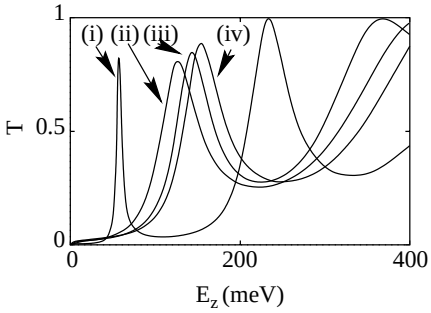

Fig. 2. The transmission coefficient T *vs.* the incident electron energy E_z for the asymmetric DBRTS shown in Figure 1 at the bias voltages (i) $v = 0$, (ii) $v = 200$, (iii) $v = 150$ and (iv) $v = 150$ mV where the nonparabolicity has been included in (iii) only. For (i), (ii) and (iv), the nonparabolicity has been ignored. The peaks of curve occur at (i) 57.5 meV and 233.6 meV. The peak occurs at (ii) 128.0 meV. The peak of curve (iii) occurs at 143.7 meV, and the peak of curve (iv) occurs at 154.0 meV.

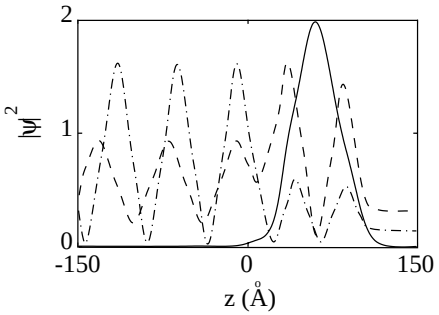

Fig. 3. Spatial dependence of the normalized electron envelope wavefunction $|\psi(z)|^2$ throughout the same DBRTS as in Figure 1 with the bias v =150 mV for electron energies: $E_w = -24.05$ meV (the confined state in the well represented by a solid line), $E_z = 154$ meV (the second resonant state represented by a dashed line) and $E_z = 200$ meV (the off-resonant state represented by a dash-dot line). The scale is 10^{-2} Å^{-1} for the solid line and 10^{-3} Å^{-1} for the dashed and dash-dot lines.

a bias voltage $v = 0$. The first transmission peak occurs for an incident energy equal to the resonance energy of the well. The second transmission peak occurs for an incident energy which is larger than the energy of the first barrier. However, a resonance energy of 233.6 meV exists because the electron is reflected by the second barrier and also undergoes a quantum reflection from the first barrier, which is analogous to the Ramsauer effect [30]. The peak shifts towards low energy as the bias voltage increases. For instance, the second peak is moved to $E_z = 154$ meV and the first level $E_1 = E_w \doteq -24.05$ meV is lower than the conduction band edge of the emitter, which becomes a fully confined state in the well at the voltage $v = 150$ mV. The corresponding electron envelope wavefunctions are shown in Figure 3. The position of the peak shifts to lower energy as the bias voltage increases again. For example, the second peak is moved to $E_z = 128$ meV in the case of $v = 200$ mV. Moreover, Figure 2 also clearly indicates that the subband nonparabolicity has a large influence on the incident electron state. When considering the conduction band nonparabolicity, the value of the peak decreases slightly and the position of the peak moves again to lower energy.

In Figure 3, we show the spatial structure of the electron envelope wavefunctions on the confined state with $E_w = -24.05$ meV in the well, the second resonant state with $E_z = 154$ meV and the off-resonant state with $E_z = 200$ meV at the bias $v = 150$ mV for the asymmetric DBRTS depicted in Figure 1. The figure indicates that the resonant state is mostly contained within the QW whereas the opposite is true for the off-resonant state. The overlap integral between the confined state and the resonant state is larger than that between the confined state and the off-resonant state.

In order to study the properties of the electron-phonon interaction in asymmetric DBRTS, we investigate the dispersion of interface modes, the electron-interface-phonon interaction Hamiltonian characteristic as a function of wavenumber k and coordinate z and the electron-phonon scattering for the same asymmetric DBRTS as in Figure 1. Our numerical calculations indicate (i) that the dispersion of the interface modes is apparent for $k < 0.1$ Å^{-1}, (ii) that the electron-interface-phonon interaction Hamiltonian is a very complicated function of wavenumber k, and (iii) that the contribution of the four lower-frequency interface modes to the scattering rate is much smaller than that of the four higher-frequency interface modes. Figure 4 shows the scattering rate divided by $(N_{ph}+1)$ as a function of the incident electron energy E_z for the same structure as in Figure 1 at the bias voltage $v = 150$ mV. We can see from Figure 4 that electron-interface-phonon scattering is much more important than electron-LO-phonon scattering for low incident electron energy E_z which is approximately one order of magnitude greater than the Fermi energy level. In Figure 4 the intersection between the curves for the two scattering rates occurs at $E_z \doteq 162$ meV, which is approximately within one order of magnitude of the Fermi energy $E_F = 42.5$ meV corresponding to the doping concentration $n = 1 \times 10^{18}$ cm^{-3} at the temperature $T = 300$K. The electron-LO-phonon scattering is evidently much more important for $E_z > 162$ meV. Figure 4 also clearly shows that the total scattering rate has a maximum at $E_z \doteq 154$ meV. The reason is simple. We know from Figures 2 and 3 that $E_z = 154$ meV corresponds to the second resonant level at $v = 150$ mV. The overlap intergral between the confined state in the well and the second resonant state has the largest value. Hence, the electron-phonon scattering rate has a maximum at $E_z = 154$ meV according to equations (2.21, 2.22).

The relationship between the total scattering rate and the different bias voltage has also been investigated. Figure 5 clearly shows that the influence of the bias voltage on the electron-phonon scattering rate has two aspects. One is the position of the scattering peak moves to the low energy when the voltage increases. The other is the value of the peak decreases if the voltage increases. We know from Figure 2 that the second resonant energy level decreases when the voltage increases. Hence, the peak scattering

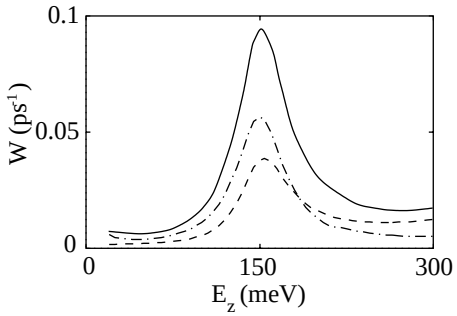

Fig. 4. The electron-phonon scattering rate W divided by $(N_{ph}+1)$ as a function of the incident electron energy E_z for the structure in Figure 1 at the bias voltage $v = 150$ mV. The dash-dot line represents the contribution of the interface phonons, and the dashed line represents the confined bulk-like LO phonons. The solid line represents the total scattering rate. The peaks occur in close proximity to the quantum well resonance.

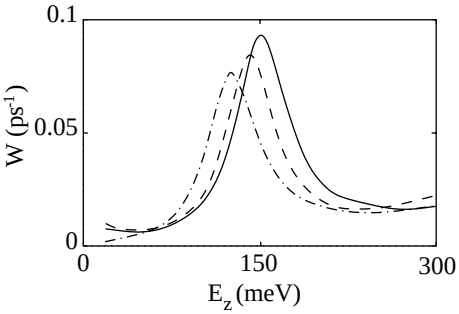

Fig. 5. The total scattering rate W divided by $(N_{ph}+1)$ as a function of the incident electron energy E_z for the structure in Figure 1 at the voltage $v = 150$ mV (the solid line ignores nonparabolicity and the dashed line includes nonparabolicity) and $v = 200$ mV (the dash-dot line ignores nonparabolicity).

rate shifts towards lower energy, and the decreasing peak value is due to the decreasing overlap integral between the incident electron state and the confined state in the well as the bias voltage increases. In order to further investigate the influence of the conduction band nonparabolicity on the electron-phonon scattering, we have calculated the electron-phonon scattering rate in considering the subband nonparabolicity for the same DBRTS as in Figure 1 at the bias voltage $v = 150$ mV in Figure 5. This figure shows that the subband nonparabolicity has a large influence on the electron-phonon scattering, which is similar to the influence of the nonparabolicity on the transmission coefficient shown in Figure 2.

It is worthwhile to further analyse the physical implications with respect to the two transmission peaks shown in Figure 2. First, we know from the coherent tunneling theory [1] that the coherent tunneling current in DBRTS can be completely determined by the height of the resonant level, the peak value of the transmission coefficient $T(E_z)$ on the resonant level and the position of the transmission peak. Hence, the two transmission peaks of Figure 2 will have a significant influence on the coherent tunneling process in our DBRTS. They will directly control the coherent tunneling current-voltage characteristic, which is very important for designing better resonant tunneling diodes. Moreover, we know from Figures 4 and 5 that the electron-phonon scattering rate has its maximum if the incident electron energy is near the second resonant level. This is also very important for further understanding the phonon-assisted tunneling process in DBRTS, which has attracted much attention in recent years [6–18].

4 Summary

In this paper, we present a general theory for electron states in an arbitary potential field by using a transfer matrix method. As an application of our theory, the electron transmission coefficient and the envelope wavefunction in asymmetric DBRTS are calculated. The electron-phonon interaction and scattering in an asymmetric DBRTS is studied based on the dielectric continuum model, in which all of the phonon modes are included. The conduction band nonparabolicity is also considered. We give our numerical results for the electron transmission coefficient, the electron envelope wavefunction and the electron-phonon scattering rate in asymmetric DBRTS GaAs/$Al_{0.25}Ga_{0.75}As$/GaAs/$Al_{0.3}Ga_{0.7}As$/GaAs with thickness 1000 Å/30 Å/60 Å/20 Å/1000 Å at different bias voltages. The importance of the different phonon modes is analyzed. Our main conclusions are summarized as follows.

1. The electron-phonon scattering rate, the electron transmission probability and the electron envelope wavefunctions depends sensitively on the incident electron energy and on the bias voltage.
2. The electron-phonon scattering rate is maximised for the incident electron energy near the second resonant level, which is very important for understanding the phonon-assisted tunneling process in DBRTS.
3. Higher-frequency interface modes are much more important than lower-frequency interface modes for the electron-phonon interaction and scattering in DBRTS.
4. Interface modes are much more important than confined bulk-like LO phonons when the incident electron energy is small. Otherwise, the confined LO phonons become much more significant if the incident electron energy is large.
5. The subband nonparabolicity has a significant influence on the electron transmission and the electron-phonon scattering in DBRTS.

The scattering rates observed in Figures 4 and 5 reveal that, for the structure in Figure 1, the relaxation time is on the order of 10 to 100 ps. It is interesting to compare this timescale with the dwell time in the DBRTS. The dwell time in a symmetric $Al_{0.4}Ga_{0.6}As$/GaAs/$Al_{0.4}Ga_{0.6}As$ with a well height of 50 Å is also on the order of 10 to 100 ps [31]. Although a different result for the dwell time is expected for an asymmetric structure, the electron dwell time and the relaxation time are comparable.

The theoretical results obtained in this paper are useful for further investigations of phonon-assisted tunneling in DBRTS, particularly with respect to decoherence and scattering in resonant tunneling devices.

Jun-jie Shi has been supported by an Overseas Postgraduate Research Scholarship and a Macquarie University International Postgraduate Research Award. This work has been supported by an Australian Research Council Large Grant and by a Macquarie University Research Grant. We have benefitted by many useful discussions with L. Tribe, E.M. Goldys, D.J. Skellern, and G.J. Milburn, and we thank L. Tribe for preparation of the figures.

References

1. R. Tsu, L. Esaki, Appl. Phys. Lett. **22**, 562 (1973).
2. L.L. Chang, L. Esaki, R. Tsu, Appl. Phys. Lett. **24**, 593 (1974).
3. T.C.L.G. Sollner, W.D. Goodhue, P.E. Tannenwald, C.D. Parker, D.D. Peck, Appl. Phys. Lett. **43**, 588 (1983).
4. E.R. Brown, T.C.L.G. Sollner, C.D. Parker, W.D. Goodhue, C.L. Chen, Appl. Phys. Lett. **55**, 1777 (1989).
5. H. Mizuta, T. Tanoue, *The Physics and Applications of Resonant Tunnelling Diodes* (Cambridge University Press, Cambridge, 1995).
6. V.J. Goldman, D.C. Tsui, J.E. Cunningham, Phys. Rev. B **36**, 7635 (1987).
7. N.S. Wingreen, K.W. Jacobsen, J.W. Wilkins, Phys. Rev. Lett. **61**, 1396 (1988).
8. M.L. Leadbeater, E.S. Alves, L. Eaves, M. Henini, O.H. Hughes, A. Celeste, J.C. Portal, G. Hill, M.A. Pate, Phys. Rev. B **39**, 3438 (1989).
9. M. Jonson, Phys. Rev. B **39**, 5924 (1989).
10. W. Cai, T.F. Zheng, P. Hu, B. Yudanin, M. Lax, Phys. Rev. Lett. **63**, 418 (1989).
11. F. Chevoir, B. Vinter, Appl. Phys. Lett. **55**, 1859 (1989).
12. N.S. Wingreen, K.W. Jacobsen, J.W. Wilkins, Phys. Rev. B **40**, 11834 (1989).
13. P.J. Turley, S.W. Teitsworth, J. Appl. Phys. **72**, 2356 (1992).
14. P.J. Turley, S.W. Teitsworth, Phys. Rev. B **44**, 3199 (1991); *ibid.* **44**, 8181 (1991); *ibid.* **50**, 8423 (1994).
15. N. Mori, K. Taniguchi, C. Hamaguchi, Semicond. Sci. Technol. **7**, B83 (1992).
16. N. Zou, K.A. Chao, Phys. Rev. Lett. **69**, 3224 (1992).
17. P.J. Turley, S.W. Teitsworth, Phys. Rev. B **44**, 12959 (1991).
18. Li-jun Liu, Yuan-tai Du, Hong Zhou, Tsung-han Lin, Phys. Rev. B **54**, 1953 (1996).
19. Jun-jie Shi, Shao-hua Pan, Phys. Rev. B **51**, 17681 (1995).
20. Jun-jie Shi, Shao-hua Pan, J. Appl. Phys. **80**, 3863 (1996).
21. Jun-jie Shi, Xiu-qin Zhu, Zi-xin Liu, Shao-hua Pan, Xing-yi Li, Phys. Rev. B **55**, 4670 (1997).
22. J. Chen, J.G. Chen, C.H. Yang, R.A. Wilson, J. Appl. Phys. **70**, 3131 (1991).
23. T. Schmidt, M. Tewordt, R.J. Haug, K.V. Klitzing, B. Schönherr, P. Grambow, A. Förster, H. Lüth, Appl. Phys. Lett. **68**, 838 (1996).
24. P. Orellana, F. Claro, E. Anda, S. Makler, Phys. Rev. B **53**, 12967 (1996).
25. G. Kim, Dong-Wan Roh, S.W. Paek, J. Appl. Phys. **81**, 7070 (1997).
26. T. Schmidt, R.J. Haug, K.V. Klitzing, A. Förster, H. Lüth, Phys. Rev. B **55**, 2230 (1997).
27. G. Bastard, Phys. Rev. B **24**, 5693 (1981).
28. C. Kittel, *Introduction to Solid State Physics*, 5th edn (Wiley, New York, 1976).
29. M.O. Vassell, J. Lee, H.F. Lockwood, J. Appl. Phys. **54**, 5206 (1983).
30. R.L. Liboff, *Introductory Quantum Mechanics* (Holden-Day, San Francisco, 1980) Section 7.8.
31. H.C. Liu, T.C.L.G. Sollner, in *High Speed Heterostructure Devices Semiconductors and Semimetals*, edited by R.A. Kiehl, T.C.L.G. Sollner (Academic Press, Boston, 1994).